On the effect of the superconducting phase transition on phonons in $YBa_2Cu_4O_8$: an infrared spectroscopic study

1992 J. Phys.: Condens. Matter 4 10367

(http://iopscience.iop.org/0953-8984/4/50/025)

J. Phys.: Condens. Matter 4 (1992) 10367–10376. Printed in the UK

On the effect of the superconducting phase transition on phonons in $YBa_2Cu_4O_8$: an infrared spectroscopic study

H S Obhi†, E K H Salje† and T Miyatake‡

† IRC in Superconductivity, Madingley Road, University of Cambridge, Cambridge CB3 0HE and Department of Earth Sciences, Downing Street, University of Cambridge, Cambridge CB2 3EQ, UK

‡ Superconductivity Research Centre, International Superconductivity Technology Centre, 1-10-13 Shinonome, Koto-ku, Tokyo 135, Japan

Received 1 June 1992, in final form 15 October 1992

Abstract. Phonon spectra of $YBa_2Cu_4O_8$ have been measured in the range 110–1000 cm^{-1} and between 30 K and room temperature. All seven B_{1u}-symmetry infrared-active phonons are observed at 119, 135, 200, 314, 332, 500 and 605 cm^{-1} at 290 K. The effect of decreasing temperature on phonons with frequencies $\gtrsim$ 210 cm^{-1} has been studied and it is found that the 500, 314 and 605 cm^{-1} modes—and perhaps also the 332 cm^{-1} mode—exhibit changes in frequency, intensity and linewidth at the superconducting transition temperature (80 K). The observed phonon renormalization effects are compared to those previously observed in $YBa_2Cu_3O_{7-\delta}$. Our results suggest that polaron–phonon interactions may be important for the occurrence of superconductivity in these materials—e.g. via the Bose condensation of bipolarons.

1. Introduction

The behaviour of phonons in high-temperature superconductors is of great significance as dynamic lattice effects in general, or phonons in particular, may play a relevant role in the mechanism underlying superconductivity in these compounds [1–3]. Equally important is the empirical observation that changes in the phonon self-energy and the dielectric response function provide a powerful tool for the experimental investigation of the superconducting phase transition. Indeed, phonon frequencies and absorption cross sections vary significantly with the superconducting order parameter and allow for a quantitative determination of its dependence on temperature, doping, etc [4–8]. Furthermore, mixed phonon–plasmon [9, 10] and phonon–polaron excitations [2, 11, 12] appear in the infrared spectrum of high-temperature superconductors. Their relevance lies in their observed renormalization with the onset of superconductivity in $YBa_2Cu_3O_{7-\delta}$ (hereafter referred to as 123).

We now turn our attention to the phononic excitations. In contrast to most conventional superconductors, the lower carrier concentration in copper oxide superconductors allows direct measurement of (k = 0) optical phonons using infrared spectroscopic techniques. Recent infrared and Raman studies of 123 shows that changes in phonon frequency and intensity at the superconducting transition temperature, T_c correlate directly with the order parameter in the superconducting state [4, 5 and references therein]. Regardless of the details of the possible role

0953-8984/92/5010367+10$07.50

of phonons in the microscopic mechanism of high-T_c superconductivity, it is clear that, in 123 at least, phonon renormalization effects at T_c are a useful probe of the superconducting state, even to elucidate fluctuation phenomena above T_c in 123 [4]. The following question arises from these observations: is the success of the phonon-spectroscopic method for the investigation of superconductivity an exception which applies only for the 123 structure? A good argument why this might be the case relates to the geometrical significance of the apical oxygen and the closeness of the electronic structure of the CuO chains to the Fermi energy, E_F [13–15]. Both features could increase the coupling between the superconducting order parameter and phonons with amplitudes mainly related to chain atoms and/or the apical oxygen.

In order to study these effects, we repeat our investigations of 123 on the 80 K superconductor $YBa_2Cu_4O_8$ (hereafter referred to as 124). These materials are structurally closely related, the main difference being an extra CuO chain in 124 that is shifted by $b/2$ and is parallel to the CuO chain in 123, thus forming a ribbon-like arrangement in the bc-plane (figure 1). Hence, the length of the unit cell of 124 (c = 27.19 Å [16]) is just over twice that of 123. In contrast to 123, 124 possesses no apical oxygen between the ribbon and CuO_2 planes and the ribbon states in 124 are further below E_F than the chain states in 123 [5].

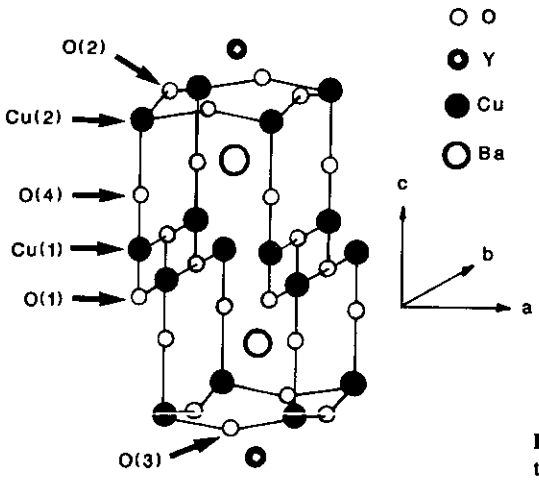

Figure 1. The structure of $YBa_2Cu_4O_8$ showing the labelling of atoms referred to in the text.

Technologically, 124 is interesting because it displays a lesser degree of orthorhombicity than 123 (a = 3.842 Å, b = 3.863 Å in 124 [16] and a = 3.819 Å, b = 3.885 Å in 123 [7] and does not exhibit crystal twins. Furthermore, the stability of the CuO ribbons—Cu(1) in square-planar coordination, O(1) in threefold symmetry—results in a fixed oxygen stoichiometry. Due to their homogeneous relationship, 124 is a useful material to compare and contrast with 123.

Previous infrared spectroscopic work on 124 [18–21] were conducted using reflection techniques. An investigation of the temperature dependence of infrared-active phonons in 124 is reported in the excellent paper by Litvinchuk *et al* [22]. We show in this paper that there is substantial agreement between their reflection measurements and our absorption studies. Buckley *et al* [18] did not measure temperature effects, although their interesting studies on the effect of La substitution assisted them in suggesting phonon assignments. Ziaei *et al* [19] studied the far-

and mid-infrared reflectance of 124 at temperatures above and below T_C, but did not perform a Kramers–Krönig analysis of their spectra. By investigating a wide frequency range (mid-infrared to UV), Bucher *et al* [20,21] measured considerable anisotropy in the reflectance and frequency-dependent conductivity of single crystals. However, individual phonon modes were not clearly resolved. On the other hand, infrared absorption spectroscopy allows the direct observation of phonon frequencies and their absorption profiles, thus avoiding indirect profile-evaluation methods (e.g. Kramers–Krönig) and any of the associated errors that can arise in such analyses. For example, the use of Drude-type extrapolations to approximate background functions is not accurate and can seriously influence the fitting of dielectric functions [9,20]. Most of these experimental problems can be overcome if the direct absorption/transmission spectrum is measured. The difficulty of this method, however, is a weak dependence of the peak positions on the embedding material (see pellet preparation in section 2) such that the peak positions are slightly shifted from the true TO frequency towards the LO frequency. This effect has to be borne in mind for any comparisons to absolute frequencies, although the effect was found to be small in 123. Here we are interested in the *relative* changes of the phonon signals with the onset of superconductivity and it is generally thought that there is virtually no influence from the embedding material on such data.

2. Experimental details

$YBa_2Cu_4O_8$ samples were prepared using a high-oxygen-pressure synthesis. Details of the procedure and subsequent characterization methods used, including x-ray analysis, resistance and magnetic measurements are described elsewhere [16].

After being ground in a Spex electrical mill, the powdered superconductors—approximately 0.1 μm diameter grains—were mixed with dry CsI and pressed (at 10 tons cm^{-2}) into disc-shaped pellets of 13 mm diameter at room temperature. Each pellet contained 2 mg of superconductor and identical pellets of the CsI diluent were used as references. All pellets were stored under dry, cool conditions (dessicator, silica gel) and measured within 12 h of production.

A Bruker 113v FTIR spectrometer set at 2 cm^{-1} resolution (utilizing liquid-nitrogen-cooled MCT and DTGS detectors) was used for the absorption measurements. Spectra were recorded in the mid- and far-infrared under vacuum with the pellet in a Leybold He-cryostat equipped with KRS-5 windows, thus allowing a range from 30 K to room temperature to be achieved. An Aspect 3000 computer was used for the data collection and data analysis was performed by this computer and also on a PC served by the Aspect via an IEEE interface. A least-squares band-profile analysis of the spectra was conducted using Voigt profiles, enabling the absolute frequency of each phonon band to be directly estimated from the spectrum with a random error in measurement of ± 0.5 cm^{-1}. Spectral subtraction and integration was also performed, as will be described in the following section.

3. Results and discussion

3.1. The non-superconducting phase at room temperature

The infrared absorption spectra of 124 were first measured at room temperature (290 K) (figure 2). We find strong phonon resonances at 119, 135, 314, 332, 500

and 605 cm^{-1}. In addition, weaker modes are observed at 200 (broad), 236, 449 (broad), and 558 cm^{-1}. At higher frequencies, tiny traces of $BaCO_3$ impurity phase, at ~690 cm^{-1} and ~857 cm^{-1}, are identified and this may also be the origin of the mode at 236 cm^{-1}. As the major phonon lines in all spectra are fairly sharp, it is evident that the structure is reasonably well ordered [16].

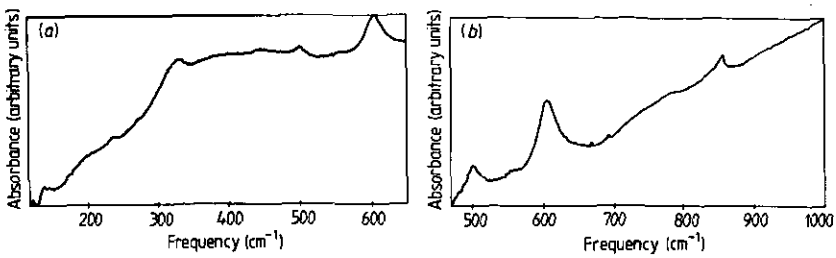

Figure 2. Infrared absorption spectra of $YBa_2Cu_4O_8$ at room temperature.

Orthorhombic 124 has space group *Ammm* with the following optically active, irreducible representation: $7(A_g + B_{2g} + B_{3g} + B_{1u} + B_{2u} + B_{3u})$. Lattice-dynamical calculations within a shell-model description [23] predict the frequencies for $k = 0$ Raman-active, LO and TO infrared-active modes. The high ab-plane conductivity obscures the B_{2u} and B_{3u} lattice vibrations, leaving just seven B_{1u} infrared-active modes observable. The broad, weaker peaks seen at 449 and 558 cm^{-1} may possibly be due to impurities. It is, however, also feasible that these are B_{2u} ($\| a$) modes. The B_{3u} ($\| b$) modes are much more likely to be screened by the higher conductivity parallel to the ribbons. Table 1 shows the correspondence of our measurements with previous infrared work and the lattice-dynamical calculations mentioned above.

Table 1. A comparison of estimates of B_{1u}-symmetry phonon frequencies (all values are in cm^{-1}).

Shell-model calculations [23]	*IR reflectance* [19]	*IR reflectance and KK analysis* [18]	*IR reflectance and KK analysis* [22] (frequencies at 10 K)	*IR absorption* (this work)	*Major ion motions*
121		111	133	119	Cu(2), Ba
150	130	129	162	135	Complex, 'Ba-mode'
193	192(weak)	190(weak)	192	~200(weak)	Y
259	~315	282	236	314	Out of phase O(2),O(3)
364	~337	307	304	332	In phase O(2),O(3), complex
512	500	496	493	500	O(1)
598	603	600	599	605	O(4) and out of phase O(1)

Buckley *et al* [18] report seven modes in infrared reflection (and also find traces of $BaCO_3$). In general, their phonon frequencies are a few wavenumbers lower than ours (table 1). The possibility of such a large systematic error in our frequency

measurements can be ruled out, since the $BaCO_3$ lines appear at their generally accepted frequencies. Another consideration is the difference in the reflection and transmission techniques. It is possible, therefore, that the discrepancy in frequencies could originate from the embedding process shifting our frequency estimate towards higher LO frequencies or perhaps errors arising out of Kramers–Krönig analysis of the reflectance spectra. In terms of absolute frequencies, our results are in much better agreement with the measurements of Ziaei *et al* [19] (table 1) who identified six modes in reflection (they did not observe the mode near 119 cm^{-1}). Seven modes were reported by Litvinchuk *et al* [22] and their determinations of the two highest phonon frequencies concur well with ours. Although their measurements show no clear resolution of the two phonons at 314 cm^{-1} and 332 cm^{-1}, they do however, observe asymmetry (high-frequency wing) in the feature they see at ~310 cm^{-1}. (They also report an asymmetry in the 493 cm^{-1} phonon profile, but this is not apparent in our spectra.) Their observation of a peak at 236 cm^{-1} is in agreement with our results, but whilst we suggest that this originates from the $BaCO_3$ traces, they assign this phonon to a B_{1u} symmetry mode in 124.

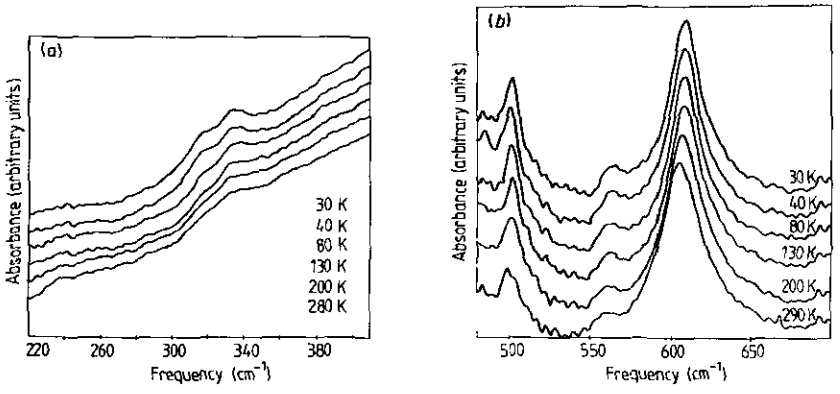

Figure 3. Absorption spectra at various temperatures above and below T_c (= 80 K).

3.2. The effect of temperature

Phonon spectra at temperatures above and below T_c are shown in figure 3. As the temperature is lowered from 290 K, the frequency of the phonon at 500 cm^{-1} first increases at $d\tilde{\nu}/dT \approx -9.9 \times 10^{-3}$ cm^{-1} K^{-1}. Near T_c the frequency decreases sharply by ~2 cm^{-1} (figure 4(*a*)). Ziaei *et al* [19] reported similar behaviour, but did not quantify their observations. The temperature dependence of the integrated intensity of the phonon near 500 cm^{-1}, which primarily involves motion of O(1) in the ribbons, is shown in figure 4(*b*). As the temperature is lowered, the integrated intensity remains fairly constant for $T > T_c$. Below T_c the intensity increases markedly. The full width at half-maximum (FWHM) of this phonon narrows uniformly with decreasing temperature to T_c at a rate of $\approx 2.2 \times 10^{-2}$ cm^{-1} K^{-1} and then narrows further below T_c, but at a much reduced rate, $\sim 5 \times 10^{-2}$ cm^{-1} K^{-1}. Similar behaviour of the phonon frequency and oscillator strength was reported by Litvinchuk *et al* [22]. They estimated a slightly larger decrease in frequency of ~5 cm^{-1} as the temperature is decreased from T_c. At $T > T_c$, our measurements of the temperature

dependence of the linewidth of this phonon concur well with those in [22]; the rate of narrowing as temperature is lowered to T_c is linear and of order 10^{-2} cm^{-1} K^{-1}. However, below T_c, Litvinchuk *et al* [22] report a *change in sign* in the gradient of the linewidth against temperature, i.e. a broadening with decreasing temperature for $T < T_c$. In contrast, we measure only narrowing with decreasing temperature. Nevertheless, it is interesting to note that we also observe a reduced rate of narrowing with decreasing temperature below T_c for this phonon.

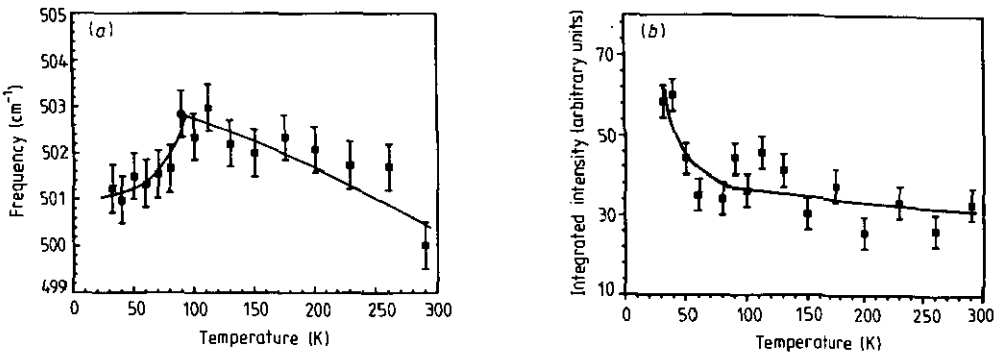

Figure 4. Temperature dependence of the 500 cm^{-1} phonon frequency (*a*) and integrated intensity (*b*). Lines are guides for the eye.

This renormalization effect of the phonon frequency is much smaller than that observed for the Cu(1), O(4) apical oxygen mode in 123 at ~575 cm^{-1} which softens by ~5 cm^{-1} on cooling from T_c [5]. In direct contrast, the phonon in 124 which primarily involves O(4), Cu(1) motion does not show any anomalous changes in frequency at T_c (figure 5(*a*)). A smooth increase in frequency is evident, from 605 cm^{-1} at room temperature, saturating to a value of 608 cm^{-1} below ~100 K. The integrated intensity of this mode decreases a little on cooling to T_c (figure 5(*b*)). However, as T approaches 0 K from T_c, it is found that the integrated intensity drops very rapidly. The linewidth of this phonon narrows linearly with decreasing temperature at 2.7 x 10^{-2} cm^{-1} K^{-1}, with no anomalous behaviour at T_c. Ziaei *et al* [19] detected no changes in the linewidth of this phonon as a function of temperature, and moreover suggested a slight *softening* of this mode on cooling. Litvinchuk *et al* [22] report no pronounced temperature dependence of this mode. In comparison, our results clearly resolve the increase in frequency, narrowing and the decrease in integrated intensity of this phonon mode as T approaches 0 K.

Integrating the baseline-corrected spectra between 280 and 360 cm^{-1} yields the total integrated intensity of *both* phonons at 314 and 332 cm^{-1} with temperature (figure 6(*a*)). As the temperature is lowered, the intensity remains roughly constant, but at T_c it begins to increase and does not appear to saturate even at $\frac{1}{3}T_c$ ($\approx$ 30 K). In order to distinguish the phonons in this doublet, at least-squares peak-profile analysis (Voigt profiles) using two peaks was carried out. It is found that the mode near 314 cm^{-1} intensifies greatly on cooling from T_c, whilst the intensity of the 332 cm^{-1} mode rises slightly with decreasing temperature and perhaps decreases a little at T_c (figure 6(*b*) and (*c*)). In addition to the above analysis, spectra taken at temperatures below T_c were subtracted from the spectrum at 100 K and the

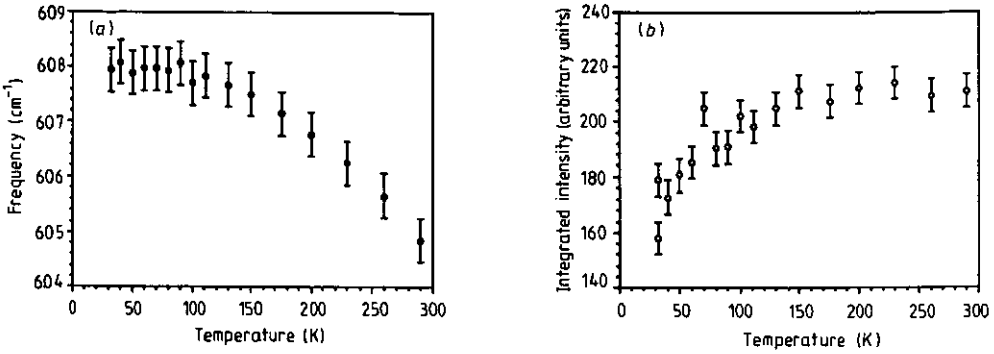

Figure 5. Temperature dependence of the 605 cm^{-1} phonon frequency (*a*) and integrated intensity (*b*).

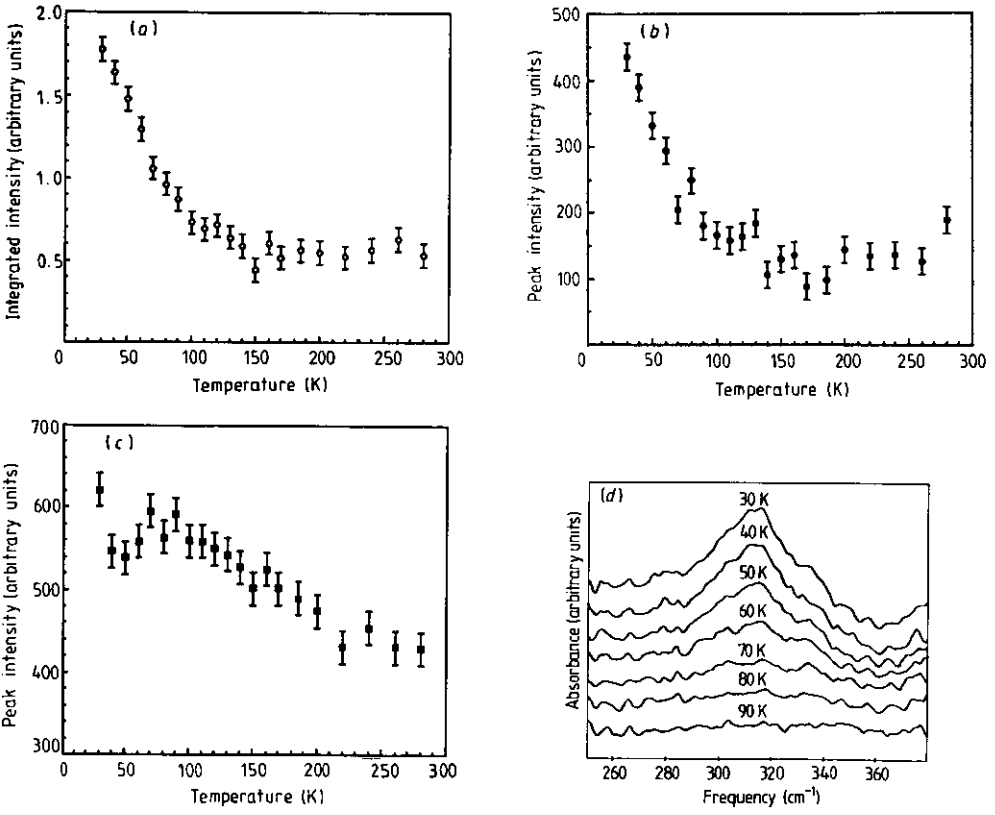

Figure 6. Temperature evolution of (*a*) of the integrated intensity of *both* phonons at 314 and 332 cm^{-1}; (*b*) peak intensity of the 314 cm^{-1}; (*c*) peak intensity of the 332 cm^{-1} mode; (*d*) difference spectra—i.e. spectrum at 100 K subtracted from spectra at temperatures indicated. Each difference spectrum is plotted over the same range of absorbance units, so that intensity changes can be compared.

resulting difference spectra are stack-plotted in figure 6(*d*). This displays graphically the large intensity changes of the 314 cm^{-1} phonon as compared to the 332 cm^{-1}

mode below T_c. Both phonon frequencies increase slightly and continuously with decreasing temperature; the 314 cm^{-1} phonon hardens by $\sim$3 cm^{-1} and the 332 cm^{-1} mode by $\sim$2.5 cm^{-1}. Within the experimental resolution of our measurements, no anomalous changes in frequency are observed around T_c. Our results for this phonon pair are very different to those of Ziaei *et al* [19], where a softening of $\sim$10 cm^{-1} of the lower frequency mode below T_c was estimated from reflectance spectra, although no Kramers–Krönig analysis was performed so that a direct comparison with our measurements is not possible. A comparison can be made between our spectra (figures 3(*a*) and 6(*d*)) and the dielectric function as calculated by Litvinchuk *et al* (figure 3 of [22]). Our measurements clearly show two phonons between 280 and 360 cm^{-1} and we suggest that their data represents the *unresolved* phonon pair. It is evident therefore, that the picture presented in [22] of one phonon narrowing, softening and intensifying below T_c actually corresponds to a large increase in intensity of only the lower frequency (314 cm^{-1}) phonon in this doublet.

In order to evaluate intensity changes in powder absorption spectra at low frequencies (below $\sim$100 cm^{-1}), it is likely that the influence of the embedding material (here, CsI) needs to be taken into account. This would be most important near T_c, where the conductivity changes are largest. The extent of this effect could in principle, be estimated using an appropriate form of effective-medium theory. At higher frequencies, (e.g. Cu–O phonon frequencies) one would expect the influence of the embedding material to be smaller, but still there is the possibility of overestimating changes in phonon intensity. In the latter case, there should be concomitant anomalous changes in the dielectric function near T_c. This would certainly be of great interest for the investigation of the superconducting mechanism in the cuprates in its own right.

Measurements of lattice parameters in 124 between room temperature and 10 K indicate no anomalies at T_c, although the thermal contraction of the unit cell is anisotropic [24, 25]. Therefore, as is the case in 123, the observed phonon renormalization effects are connected to the metal–superconductor phase transition and cannot be ascribed to a purely structural phase change. It is interesting to consider electronic structure calculations by Jaejun Yu *et al* [15], as an aid to understanding the small phonon renormalization of the 500 cm^{-1} 'ribbon mode' in 124, the absence of sharp frequency changes in the apical oxygen mode in 124 and the large intensity changes in the Cu(2)–O(2), O(3) modes in 124 with respect to similar modes in 123. In these studies, the authors showed (using all-electron local-density full-potential linearized augmented-plane-wave (FLAPW) methods) that the main contributions to the valence band density of states (DOS) come from Cu d and O p orbital interactions. The McMillan–Hopfield parameter, η, gauges the electron–phonon coupling with the coupling constant [15]

$$\lambda \simeq \sum_{j=1}^{N} \lambda_j = \sum_{j=1}^{N} \frac{\eta_j}{m_j \langle \omega^2 \rangle}$$

where the subscript j labels each atom, the sum runs over all N atoms of the unit cell and the RMS average frequency was taken to be $\langle \omega^2 \rangle^{1/2} \sim \Omega$, the Debye temperature. In 123 the main contributions to η originate from the chain atoms Cu(1)–O(1)–O(4) due to their large projected DOS at E_F, whilst in 124 the contributions of the Cu(1)–O(1)–O(4) atoms to η are reduced by a factor of approximately four [15]. This is directly associated with the smaller contributions of the O(1), O(4) atoms to the DOS

at E_F in 124, primarily because 124 does not have the flat antibonding dpπ band at E_F that is present in 123. The authors suggested that the observed more stable oxygen stoichiometry of 124 is attributable to the lower activity of the O(1) atoms in electron–phonon interactions with respect to 123. Our measurements support their results in the sense that we observe much reduced phonon frequency shifts for modes involving O(1), O(4) motions in 124 than for similar modes in 123. Indeed, the anomalous change in frequency below T_c—$\sim$5 cm^{-1} for 123 and $\sim$2 cm^{-1} for 124—is reasonable in the light of the four times smaller contribution of O(1), O(4), Cu(1) to η in 124 with respect to 123. Furthermore, Jaejun Yu *et al* [15] predict a slight enhancement of the contributions to η from Cu(2)–O(2), O(3) in 124 as compared to 123. This certainly correlates with our results for the dramatic intensity changes in the phonons on cooling from T_c.

It is evident that individual phonon modes in 124 do not follow conventional strong-coupling behaviour. For example, consideration of the Eliashberg phonon self-energy [1] predicts that the linewidth of phonons with frequencies above the gap ($\omega/2\Delta > 1.1$) should increase with decreasing temperature, whereas our results show that *all* phonons in 124 with frequencies $\gtrsim$ 210 cm^{-1} display only narrowing with decreasing temperature. This is in direct contrast to Y, Er and Tm doped 123, where the 570 cm^{-1} phonon linewidth was observed to increase below T_c [7]. Another striking phenomenon that emerges from our results is the behaviour of the 314 and 605 cm^{-1} phonons, which exhibit huge changes in intensity below T_c, but little or no changes in frequency. This behaviour cannot be due purely to phonon self-energy effects. On the other hand, phonon–polaron interactions have been shown to lead to a softening of optical phonons [26], although the details of phonon renormalization during the phase transition to the superconducting state are not clear. In his spin-bipolaron theory of high-temperature superconductivity, Mott [3] maintains that spins are intrinsically involved in the formation of bipolarons, but also agrees that phonons play a part. Both types of bipolaron condensation processes could clearly lead to changes in the integral absorption cross section of individual phonons involved in the condensation, without much affecting their frequencies.

Further work on the infrared properties of 124 and other high-T_c copper oxides is in progress, with the aim of gaining further insights into the behaviour of phonons in these remarkable materials.

Acknowledgments

HSO would like to thank Dr John Cooper (of the IRC) for supplying the samples, Dr John Loram (also of the IRC) for useful discussions and Catherine Morewood and Andrew Stapley for assistance with proofreading. This work was supported by SERC.

References

[1] Zeyher R and Zwicknagl G 1990 *Z. Phys.* B **78** 175
[2] Alexandrov A S 1992 *Physica* C **191** 115–30
[3] Mott N F 1991 *Phil. Mag. Lett.* **64** 211–9
[4] Obhi H S and Salje E K H 1992 *J. Phys.: Condens. Matter* **4** 195–204
[5] Obhi H S and Salje E K H 1990 *Physica* C **171** 547–53
[6] Gajić R, Schützmann J, Betz J, Zetterer T, Otto H H, Obermayer P E and Renk K F 1991 *Solid State Commun.* **78** 65–8

[7] Litvinchuk A P, Thomsen C and Cardona M 1991 *Solid State Commun.* **80** 257–62
[8] Güttler B, Salje E, Freeman P, Blunt J, Harris M, Duffield T, Ager C D and Hughes H P 1990 *J. Phys.: Condens. Matter* **2** 8977–83
[9] Gajić R, Salje E, Popovic Z and Dewing H 1992 *J. Phys.: Condens. Matter* **4** 9643–50
[10] Tachiki M and Takahashi S 1989 *Phys. Rev.* B **39** 293–9
[11] Dewing H, Salje E, Scott K and Mackenzie A 1992 *J. Phys.: Condens. Matter* **4** L109–14
[12] Salje E and Güttler B 1984 *Phil. Mag.* **50** 607–20
[13] Müller K A 1990 *Z. Phys.* B **80** 193–201
[14] Mustre de Leon J, Batistić I, Trugman A, Bishop A R and Conradson S 1992 *Phys. Rev. Lett.* **68** 3236
[15] Jaejun Yu, Key Taeck Park and Freeman A J 1992 *Physica* C **172** 467–76
[16] Miyatake T, Gotoh S, Koshizuka N and Tanaka S 1989 *Nature* **341** 41–2
[17] Schmahl W W, Putnis A, Salje E, Freeman P, Graeme-Barber A, Jones R, Singh K K, Blunt J, Edwards P P, Loram J and Mirza K 1989 *Phil. Mag. Lett.* **60** 241–8
[18] Buckley R, Staines M and Trodahl H 1992 *Physica* C **193** 33
[19] Ziaei M E, Clayman B P, Buckley R G and Staines M P 1991 *Physica* C **176** 242–6
[20] Bucher B, Karpinski J, Kaldis E and Wachter P 1992 *Phys. Rev.* B **45** 3026–36
[21] Bucher B, Karpinski J, Kaldis E and Wachter P 1990 *Physica* C **167** 324–34
[22] Litvinchuk A, Thomsen C, Murugaraj P and Cardona M 1992 *Z. Phys.* B **86** 329–35
[23] Yim K K, Oitmaa J and Elcombe M M 1991 *Solid State Commun.* **77** 385–8
[24] Alexandrov O V, Francois M, Graf T and Yvon K 1990 *Physica* C **170** 56–8
[25] Ludwig H A, Fietz W H, Dietrich M R, Wuhl H, Karpinski J, Kaldis E and Rusiecki S 1990 *Physica* C **167** 335–8
[26] Alexandrov A and Capellmann H 1991 *Phys. Rev.* B **43** 2042–9